Characterising patients and controls with brain graphs constructed from fMRI data

September 28, 2012

Supervisors:
Mason Porter
Sang Hoon Lee

Melissa Lever
Systems Biology DTC
University of Oxford

Abstract

Network science is a novel method of investigating the structure and function of the brain. We used network analysis in an attempt to distinguish between brain graphs constructed from fMRI data from patients and controls. The nodes in the brain graphs are spatial regions of interest and the strength of their connection is the correlation of the blood oxygen level-dependent (BOLD) signal of pairs of nodes. The first data set contained little temporal information, so we performed a spectral clustering method on the communicability networks generated from the data. We found that there was some distinction between healthy and brain-damaged individuals. The second data set contained time-series data, which allowed us to construct time-dependent adjacency matrices. The patients were diagnosed with schizophrenia, and the data was taken with the patients and controls taking the drugs Aripiprazole, Sulpiride, or a placebo. We performed time-dependent community detection on the multilayer networks and the mean flexibility of the network was found. We found that for all drugs, the controls had a higher mean network flexibility than the patients.

1 Introduction

The application of network science to neuroscientific data offers a novel way of investigating the structure and function of the brain. A benefit of network science is that it can be used as a framework to study a variety of disciplines. It has been found that graphs constructed from data from disparate scientific fields can have similar organisational properties and parameters, and so network science has been successfully applied to information science, biology, and many other areas [4]. Brain graphs can be constructed from a wide range of modalities including neuroimaging data (MRI and fMRI), electroencephalography (EEG) data, and magnetoencephalography (MEG) data. The abstract tools of network science are useful for summarising often large data sets to identify key features and important brain regions [17].

This report details an investigation on brain graphs constructed from fMRI data from healthy and unhealthy individuals. The first data set contains no temporal information, and I apply the graph measure of communicability [8]. The second data set contains temporal information and I apply dynamic community detection [18]. Such measures of the organisation of a brain graph allow the geometry of one functional brain graph to be compared to another. Communicability is a measure of the ease of information flow around a network that takes into account the non-shortest paths between nodes as well as the geodesics [6]. Spectral clustering on communicability networks has been shown to distinguish between fMRI data from stroke victims and healthy individuals [7], and has also revealed the brain regions responsible for the dissimilarity in networks.

Communities are mesoscopic structures in the network that are defined as groups that contain nodes that are more densely connected amongst themselves, with sparser connections between groups. This measure has been developed in order to investigate the evolution of community structure in time dependent and multiscale networks [18].

1.1 Transforming neuroimaging data to brain graphs

Graph data is presented in the form of nodes that are associated by edges, the magnitude of which describes the connection between the nodes, such as the coherence or correlation. This connectivity can be summarised in the form of an adjacency matrix $\mathbf{A}$, where $A_{ij} \in [0, 1]$ and is the strength of the edge between node i and node j. Various processing steps must take place to represent real-world neuroscientific data as a structural or functional brain graph [4].

A structural brain graph that represents the anatomy of the brain can be generated by modalities such as diffusion tensor imaging and histology. A functional brain graph measures the functional connectivity of the brain and EEG, MEG and fMRI are used as modes of data acquisition [5]. In this report we will be focussing on functional brain graphs. Graph representations of human brains are only an approximation of the underlying system, as these methods do not detect the activity of single neurons. The term coined for the complete map of structural and functional neural connections *in vivo* is the *connectome* [22]. The only species to have a complete connectome is *C. elegans*, which has around 300 neurons and 7,600 synaptic edges [5]. The human connectome by comparison has been estimated to have 10^{11} neurons and 10^{14} synapses [25].

Nodes represent brain regions, and ideally they should be independent and internally coherent in terms of anatomy or function, depending on whether a structural or functional network is being created. Functional nodes are defined from fMRI data using brain mapping methods and parcellation schemes. This is the delineation of the brain into parcels using a common approach or set of criteria [9]. The choice of parcellation scheme is influential on the resulting network properties, as is the choice in defining the connectivity between nodes [5]. The data used in this study has defined nodes as spatial regions of interest (ROIs). The activity at each node is measured as blood oxygen level-dependent (BOLD) signals.

The edges between nodes are generated by measuring the association between nodes, which could be by measuring the correlation or coherence between time series of pairs of nodes. Choices can also be made when producing the adjacency matrix. Once the connectivity between the nodes has been found, the connection between nodes can be tested for significance and then thresholded such that $A_{ij} < \tau = 0$. It is also possible to have binary adjacency matrix such that $A_{ij} \geq \tau = 1$[5]. Although

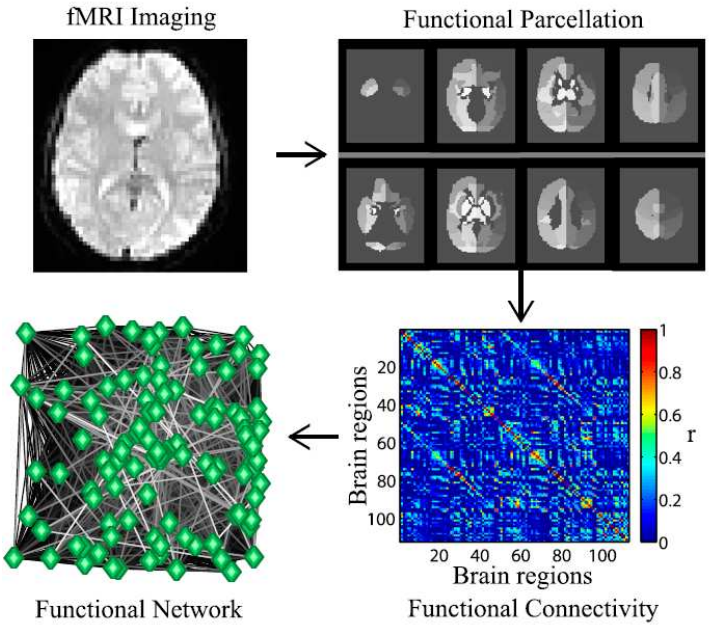

Figure 1: Multiple steps are needed to go from data acquisition to producing the final functional brain graph, and each choice has effects on the final network. Once the method of brain measurement has been chosen, the next step is to define the network nodes. In the case of fMRI, this can be done using parcellation schemes. This is the delineation of the brain into parcels using a common approach or a set of criteria [9]. The association between nodes must be calculated; with fMRI data this can be done by measuring the pairwise correlation in BOLD (Blood Oxygen Level-Dependent) signal. The resulting network can be presented in a weighted form or be thresholded to produce a binary matrix. This figure is from Ref. [17] and is used with permission.

this simplifies the adjacency matrix, it also results in a loss of information. The data sets used in this study have been thresholded and kept as weighted. Since the edges were defined through measuring correlation, the resulting matrices are symmetric, but there are ways of measuring the connectivity that results in a directed network, such as Granger causality and Bayes net methods [24].

The potential for the modality of the neuroscientific data, the experimental design, preprocessing steps, and network construction to affect the resulting brain graph means that comparison between results from analysing brain graphs from different data sets must be treated with caution.[14]

1.2 Dynamic communities

The brain is a dynamic complex system that evolves over multiple time scales. It exhibits phase-locked electromagnetic oscillations over a range of frequencies [5]. To put the time scales into perspective, the firing of an action potential in a neuron takes

about 100ms, while plastic change in synaptic strength operates over time scales of minutes to hours, and repair in cognitive function after brain damage occurs over a duration of years. It is therefore necessary to measure the dynamics of the brain over different time scales to gain a more complete understanding of the system. A necessary prospect for brain graph analysis is to model how brain functional network topology and geometry changes over time [4].

One method for investigating the time evolution of networks is to quantify how community structure changes over time. Communities can be defined as groups in a network that contain nodes that are more densely connected amongst themselves, with sparser connections between groups. One way to estimate community structure in a network is through optimising a quality function. Although community structure was initially applied to static networks, the methodology has been extended to find community structure in time dependent and multiplex networks [18]. These are networks that consist of layers of adjacency matrices. In this case, the quality function is optimised through considering *interlayer* and *intralayer* couplings between nodes. Intralayer couplings are connections between different nodes on the same network layer. Interlayer couplings are those between the same node on different network layers. The network layers can encode connections of a different type, of different scales, or of different time points.

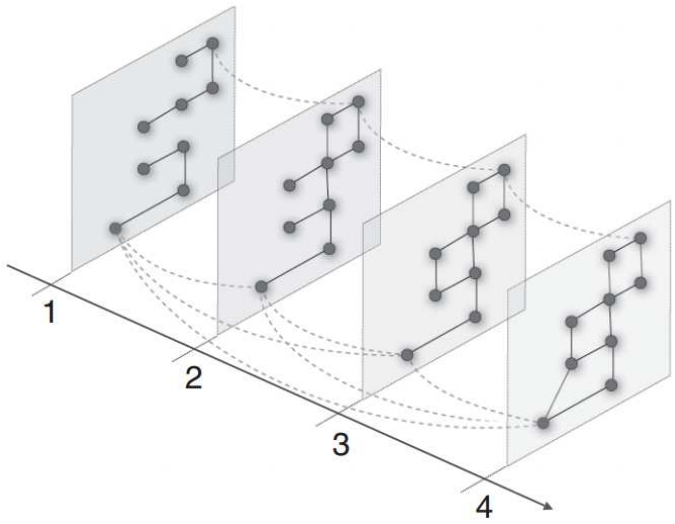

Figure 2: Community detection in multilayer networks. By introducing interlayer couplings, communities can be found that span network layers. The network layers can represent connections at different time points or of a different type. This figure is from Ref. [18] and is used with permission.

To quantify fluctuations in community structure in a network, a measure of *flexibility* can be used. This can be defined as the number of times that each node changes allegiance to a community [17]. It has been found that flexibility of a brain graph

from fMRI scans is a predictor of human learning [17].

2 Background on the data sets

2.1 Cornell data set

The first data set I used for this report was provided by the lab of Dr. Nicholas Schiff, Cornell University. It contains correlation matrices from the time series of a BOLD signal for 90 ROIs (regions of interest) from resting fMRI scans from 7 individuals, 5 of whom were healthy and 2 of whom had brain damage. Each individual had image acquisition taken at 2–4 different points in time, with some of the time intervals as large as a year. There are therefore 2–4 sets of correlation matrices per individual. There were between 88–90 nodes in each correlation matrix. However, because comparative network analysis is difficult for graphs containing different nodes, I used only the common ROIs (84 in total). Both patients regain some cognitive function in their later respective time points [1].

2.2 Cambridge data set

The second data set came from the group of Ed Bullmore at the University of Cambridge. The data set consisted of BOLD fMRI time series data taken at 498 time points for 471 ROIs from 15 healthy individuals and from 12 patients diagnosed with schizophrenia [16]. There were 3 different time series for each individual corresponding to 3 types of medication: Aripiprazole, Sulpiride, or a placebo. Aripiprazole and Sulpiride are anti-psychotic drugs.

The notion of flexibility suggests a hypothesis for the Cambridge data. Symptoms of schizophrenia include difficulties in working and long-term memory, attention, executive functioning, and speed of processing. It could therefore be hypothesised that the brain graphs of Schizophrenic patients exhibit less flexibility.

3 Methodology

3.1 Core-periphery Structure

The Core-periphery algorithm was applied to the Cornell data, although no meaningful result was found. The identification of a network into a *core* and *periphery* is to define a densely connected mesoscale core, and a sparsely connected periphery, where the nodes in the core are also well connected to the periphery. A more detailed method can be found in Ref. [23].

3.2 Communicability and Spectral clustering on static networks

Communicability is a measure of information flow in a network. It takes into account the transmission of information along the non-shortest paths as well as the geodesics. It can also be seen as a way of quantifying the "connectedness" between two nodes through the existence of shared neighbours, even if an edge between the the two nodes does not exist [8]. Because the adjacency matrices used in this study are weighted, I used a method that was adapted from the method for the binary case. This is the method formulated by Crofts & Higham [6], which builds on a communicability measure for binary adjacency networks by Estrada & Hatano [8]. In order to derive a measure for communicability it is first useful to note that for a binary adjacency matrix,

$$\left(A^k\right)_{ij} = \text{the } \textit{number} \text{ of } \textit{walks} \text{ of length } k \text{ between node } i \text{ and } j$$

where *walks* is defined as a traversal along edges in a network, and the *length* is defined as the number of edges in the walk. This result is useful if we choose to see the communicability between two nodes as a function of the number of walks length $k = 1, 2, 3$, etc. Estrada & Hatano noted that if one uses a penalisation factor of $1/k!$ for walks of length k, then the communicability between nodes i and j is

$$\left(\sum_{k=1}^{\infty} \frac{A^k}{k!}\right)_{ij} = \left[\exp(A)\right]_{ij}, \tag{1}$$

where A is a binary adjacency matrix. The communicability matrix is defined as $\exp(A)$. Crofts & Higham noted that this function does not give the desired results when applied to a weighted adjacency matrix. This is because a node with high connectivity and weights can have a disproportionate influence on the resulting communicability matrix. They therefore implemented a normalisation factor for each edge A_{ij} of $\sqrt{d_i d_j}$, where $d_i = \sum_{k=1}^{N} A_{ij}$ is the strength of node i. The communicability for a weighted network can then be defined as,

$$\left[\exp\left(D^{-\frac{1}{2}} A D^{-\frac{1}{2}}\right)\right]_{ij}, \tag{2}$$

where D is the $N \times N$ diagonal degree matrix $D := \text{diag}(d_i)$. The resulting matrix $\exp\left(D^{-\frac{1}{2}} A D^{-\frac{1}{2}}\right)$ gives a symmetric communicability network.

3.2.1 Spectral clustering

Once the communicability matrices have been defined, they can be partitioned with an unsupervised clustering algorithm such as spectral clustering method specified in the paper by Higham et. al [13]. The output of the method groups the inputs based

on their similarity to each other. This method can also be applied to adjacency and degree matrices, but Crofts & Higham suggest that the that communicability matrix gives the most effective results [7].

The first step is to use the communicability matrix to build a new matrix V so that the communicability matrix data for each subject is formatted in columns. For example, if there were S communicability matrices containing M nodes, then the new data matrix V would have S columns of length $M(M-1)/2$ since an $M \times M$ communicability matrix contains $M(M-1)/2$ communicability weights. One can then construct an $S \times S$ matrix of the form $W = V^T V$, where W_{ij} can be considered the similarity between network i and network j. The method proceeds by performing eigenvalue decomposition on the Laplacian of the weight matrix. The Laplacian is defined as,

$$L = \tilde{D} - W, \tag{3}$$

where $\tilde{D}$ is an $N \times N$ diagonal matrix of the form $\tilde{D} := \text{diag}(\tilde{d}_i)$ and $\tilde{d}_i := \sum_{j=1}^{S} W_{ij}$. The resulting Laplacian is a positive semi-definite matrix. When eigenvalue decomposition is performed on the Laplacian, the smallest eigenvalue is 0, with corresponding eigenvector of $\vec{\mathbf{1}}$, the vector where all elements are equal to 1. Assuming that the second smallest eigenvalue is unique, the eigenvalues can be ordered in increasing order as $0 = \lambda_1 < \lambda_2 < \lambda_3 \leq ... \leq \lambda_N$ with orthonormal eigenvectors $\mathbf{v}^{[1]}, \mathbf{v}^{[2]}, ..., \mathbf{v}^{[N]}$. The vector $\mathbf{v}^{[2]}$ is known as the *Fiedler vector*. The Fiedler vector compresses the network data for each individual into one dimension and has the potential to differentiate between individuals. The sum of all components in the Fiedler vector must equal 1.

3.3 Time ordered community structure

3.3.1 Constructing a correlation matrix from time-series

The Cambridge data set consisted of time-series data. This can be consolidated into adjacency networks that summarise the correlations between pairs of nodes over a time window Δ. The data is presented as a set values for N ROIs $\{X_1, X_2, ..., X_N\}$ at time points $\{t_1, t_2, ..., t_f\}$ and can be converted into a set of correlation matrices by measuring the relative similarity of pairs of nodes at mutual time points over a time window $\Delta = [t_1, t_f]$. The method used is adapted from the method used in [21]. The ROIs in the data set yield the nodes in the final adjacency matrix. Defining $X_i(t)$ as the signal of ROI i at time t, one constructs for each time window of width Δ the matrix component

$$B_{ij}(t) = \sum_{\tau=t}^{t+\Delta} X_i(\tau) X_j(\tau).$$

Implementing a normalisation factor gives an adjacency matrix with component

$$R_{ij}(t) = \frac{B_{ij}(t)}{\sqrt{B_{ii}(t)B_{jj}(t)}}. \tag{4}$$

This produces a symmetric correlation matrix with elements lying in the interval [-1,1]. The Cambridge data set contains 471 ROIs with BOLD signal measured at 498 time points. The values chosen for Δ in the study are 10, 20, 25, 30, and 40. None of these values are factors of 498, and so some of the data points were not used when constructing the adjacency matrices. For example, for $\Delta = 10$ there are 49 adjacency matrices with 8 data points remaining that are not used.

3.3.2 Constructing a brain graph from correlation matrix

The values in the correlation matrix may not represent statistically significant functional relationships. To find the significant correlations, I followed the method from Ref. [17]. This involved calculating the *p-value* P_{ij} for each element in the correlation matrix R_{ij} using the `corrcoef` function in MATLAB. I then tested p-values for significance using a false discovery rate (FDR) [11] of $p < 0.05$. Any elements in P_{ij} that did not pass the FDR threshold would have the corresponding value in R_{ij} set to 0, and the resulting matrix was set to be the adjacency matrix A.

3.3.3 Community structure

Before we consider communities in multilayer networks, we begin by considering modularity in static networks. The quality function Q for the partitioning of nodes into communities is defined as [18],

$$Q = \frac{1}{2m}\sum_{ij}\left(A_{ij} - Z_{ij}\right)\delta(g_i, g_j). \tag{5}$$

where $\delta(g_i, g_j) = 1$ if nodes i and j are assigned to the same community, and 0 otherwise. $2m$ is the number of ends of edges in the entire network. Z_{ij} is the expected connection strength between nodes i and j under a *null* model. A common measure for the null model is $Z_{ij} = k_i k_j/(2m)$, where $k_i = \sum_j A_{ij}$. Z_{ij} is the expected connection strength between node i and j if the strength of each node in A is to remain the same but the connections between nodes are made at random [19]. This gives the Newman-Girvan model of modularity, defined as,

$$Q = \frac{1}{2m}\sum_{ij}\left(A_{ij} - \frac{k_i k_j}{2m}\right)\delta(g_i, g_j). \tag{6}$$

To generalise equation (6) to multilayer networks of layers $s = 1, 2, ...T$, the interlayer couplings and the intralayer couplings must be considered. The intralayer

couplings between node i and j on layer s is defined as A_{ijs}. The interlayer coupling that connects node j in layer r to itself in layer s is denoted as C_{jrs} [17]. The generalised version of the modularity for multilayer networks is then,

$$Q_{\text{multilayer}} = \frac{1}{2\mu} \sum_{ijsr} \left[\left(A_{ijs} - \gamma \frac{k_{is} k_{js}}{2m_s} \right) \delta_{sr} + \delta_{ij} C_{jsr} \right] \delta(g_{is}, g_{jr}), \tag{7}$$

where $2\mu = \sum_{ijs} A_{ij}(s) + \sum_{srj} C_{jsr}$ and is the sum of all of the edge weights in the multilayer network. The values g_{is} , m_s, and k_{is} are generalisations of the parameters g_i, m, and k_i in equation (6) to refer to a specific layer s. There is a new parameter γ, which is a resolution parameter that can have a different value for each layer but in this study was a constant for all slices. It can be seen as $\gamma = 1/t$, where t is the duration of a random walk across the network [15]. Small values of γ result in larger communities and larger values of γ result in smaller communities. The choice of $\gamma = 1$ is the default resolution for modularity. C_{jsr} can take the binary values of $\{0, \omega\}$, and is a value of the strength of the coupling between interlayer links [18].

3.4 Computation

3.4.1 The GenLouvain algorithm

The generalized Louvain MATLAB code *GenLouvain1.2* [18] was used to perform community detection. The algorithm was obtained from NetWiki, `http://netwiki.amath.unc.edu/GenLouvain/GenLouvain`. This method is an adaption of the "Louvain" method, which is a greedy optimization method and returns high quality community detection quickly [3].

3.4.2 Calculating flexibility

The flexibility of a node can be defined as the number of times that a node changes allegiance to communities in successive time layers [2]. An alternative definition is to count how many different communities the node has belonged to. For example, a node that belongs to communities 1 and 2 in successive layers in the order "1, 2, 1, 2, 1" has flexibility of 4 by the first definition and a flexibility of 2 by the second. The flexibility of the entire network is then defined as the mean flexibility for all nodes. For clarity we will call the first definition of flexibility *flexibility 1* and the second definition *flexibility 2*.

4 Results

4.1 Spectral clustering on Cornell data

I constructed a communicability matrix for each subject from the Cornell data as given in equation (2). I then followed the spectral clustering procedure as specified in section 3.2.1 for the communicability and adjacency matrices. The Cornell data set consisted of 21 subjects and 84 common nodes between them. The data matrices V_i contained either the communicability data or the adjacency data and had the dimensions of $((84^2 - 84)/2 = 3846) \times 21$.

Eigenvalue decomposition was performed on the Laplacian (eq. 3) and the resulting components from the Fiedler vector $\mathbf{v}^{[2]}$ are shown in fig. (3). Spectral clustering is partially successful at classifying healthy ('+') individuals and brain-damaged ('o') individuals, but it does not appear to completely distinguish them, as one of the components for a brain damaged subject in $\mathbf{v}^{[2]}$ lies amongst the healthy subjects. The method is also unable to show the improvement in cognitive ability for the brain-damaged subjects. For an ideal result, the $\mathbf{v}^{[2]}$ components for the later time points from the Fiedler vector from brain-damaged subjects would be clustered near the healthy individuals. It is also unclear why there is such a large jump between the vector component values for individual 15 and 16.

The results from performing spectral clustering (section 3.2.1) on the adjacency matrix is shown in fig. (4). It can been seen that the method was unsuccessful at distinguishing between healthy and brain-damaged individuals. Crofts et. al have also found that the communicability matrix works as a more successful input than the adjacency matrix when using the spectral clustering method used in this report [7].

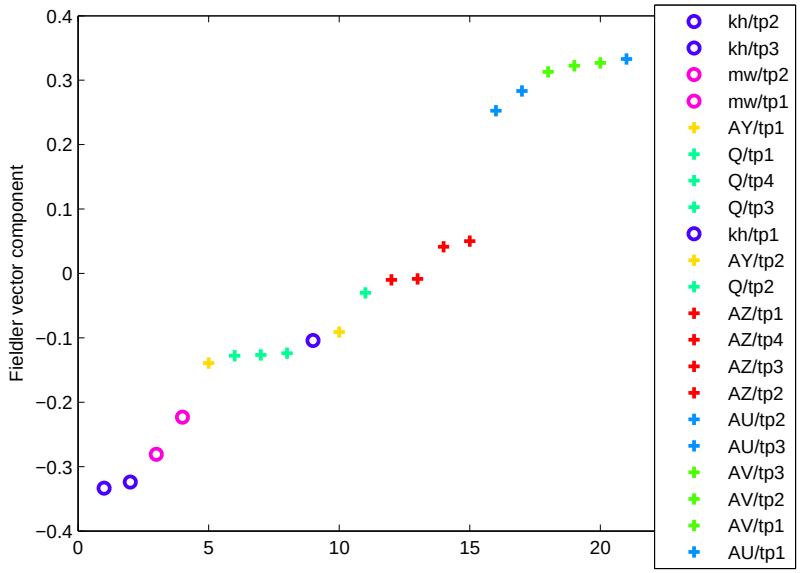

Figure 3: Components of the Fiedler vector $\mathbf{v}^{[2]}$ after performing spectral clustering as specified in Ref. [13] on communicability matrices from healthy and brain-damaged individuals. Brain-damaged individuals are shown as 'o' and healthy individuals as '+'. The method is somewhat successful in that it gives some distinction between healthy and brain-damaged. However this method fails to show that the patients increased in their cognitive ability at later time points. Spectral clustering presents one of the patients at time point 1 as being more similar to the healthy individuals

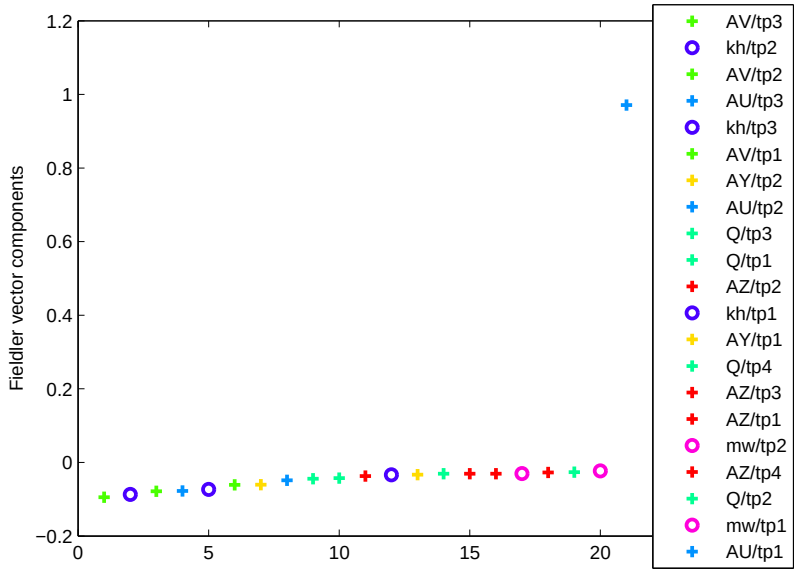

Figure 4: Components of the Fiedler vector $\mathbf{v}^{[2]}$ after performing spectral clustering as specified in Ref. [13] on adjacency matrices from healthy and brain-damaged individuals. Brain-damaged individuals are shown as 'o' and healthy individuals as '+'. Unlike spectral clustering for the communicability matrix, applying spectral clustering to the adjacency matrix does not distinguish between healthy and brain-damaged individuals.

4.2 Community structure of time-series data

I converted the time-series data into adjacency matrices by using different time windows Δ to measure the correlation between ROIs. Time windows were chosen of Δ =10, 20, 30, and 40 time points. I then ran the GenLouvain algorithm with parameters $\omega = 0.5$ and $\gamma = 0.5$ and calculated the mean flexibility of the multiplex network for each patient and control on Aripiprazole, Sulpiride and placebo. Both definitions of flexibility as defined in section 3.4.2 were used. I plot the results in fig.s (5) and (6). The results show that for both definitions of flexibility and for every choice of Δ, the controls have a higher flexibility than the patients. What is unexpected is that the antipyschotic drugs do not seem to decrease the gap in difference of flexibility between controls and patients. In fact, the largest difference in flexibility between patient and control is with the drug Aripiprazole, and this is seen most clearly with the second definition of flexibility (fig. (6)). It is interesting that controls taking Aripiprazole have a higher flexibility than when they are on a placebo, while patients on Aripiprazole show at certain values of Δ ($\Delta = 20, 30$ in fig. (5) and fig. (6)) have a lower flexibility than when they are on a placebo.

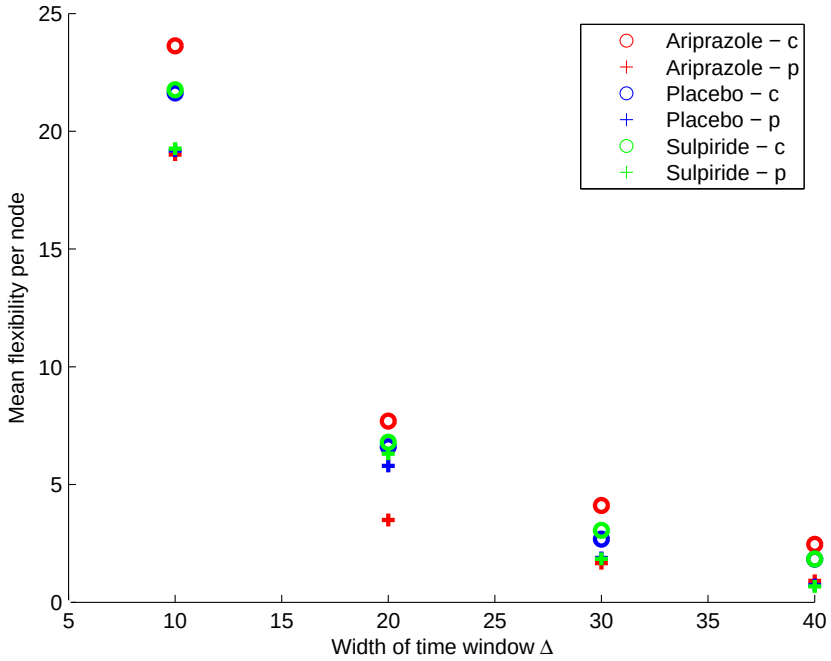

Figure 5: Mean flexibility (flexibility measure 1) per node from multilayer networks created from time-series with time windows of width Δ =10, 20, 30, 40. Patients and controls have been treated with the antipyschotic drugs Aripiprazole, Sulpiride or a placebo. It can be seen that regardless of the choice of time window width Δ, the controls have a higher flexibility that the patients

4.3 Robustness of flexibility

I found the mean flexibility from one multiplex network over a range of values of γ and ω in order to see how robust the value of flexibility is. The adjacency matrices were constructed from the time-series data from a control taking a placebo and a time window of $\Delta = 20$ was used. It is important to check whether values of flexibility are robust or are instead an artefact of the values of γ and ω. The values of ω used were in the range [0,1] and the values of γ used were in the range [0.5,10]. These were found to be values that give a reasonable community structure, for example, γ was not so small as to have each node in an isolated community or too big as to have communities that would span a network layer. Similarly, ω was large enough to have some coupling between layers but not so large that all layers were grouped into communities. I plot the results in fig. (7). It can be seen for both measures of flexibility that the value of flexibility is robust over all values of ω, while the measure flexibility 2 is not robust for $\gamma \in [0.5, 4]$.

This explains why there is a large difference between the two measures of flexibility shown in fig. (5) and fig. (6)). I used the value of $\gamma = 0.5$ in community detection,

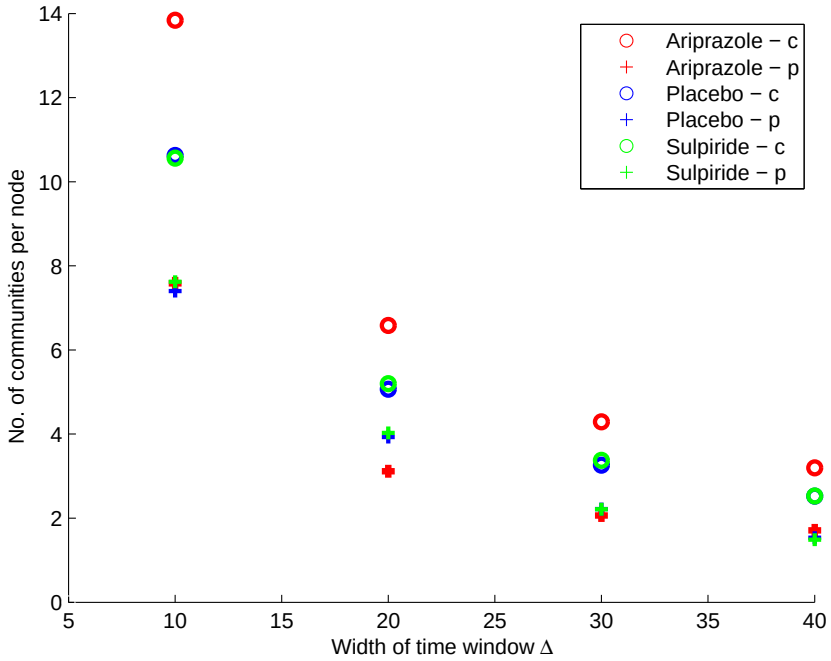

Figure 6: Mean flexibility (flexibility measure 2) per node from multilayer networks created from time-series with time windows of width Δ =10, 20, 30, 40. Patients and controls have been treated with the antipyschotic drugs Aripiprazole, Sulpiride or a placebo. It can be seen that regardless of the choice of time window width Δ, the controls have a higher flexibility that the patientsIt can be seen that the difference in flexibility between patients and controls is always greater with the drug Aripiprazole.

which we now know to be a value within which the second measure of flexibility is not robust.

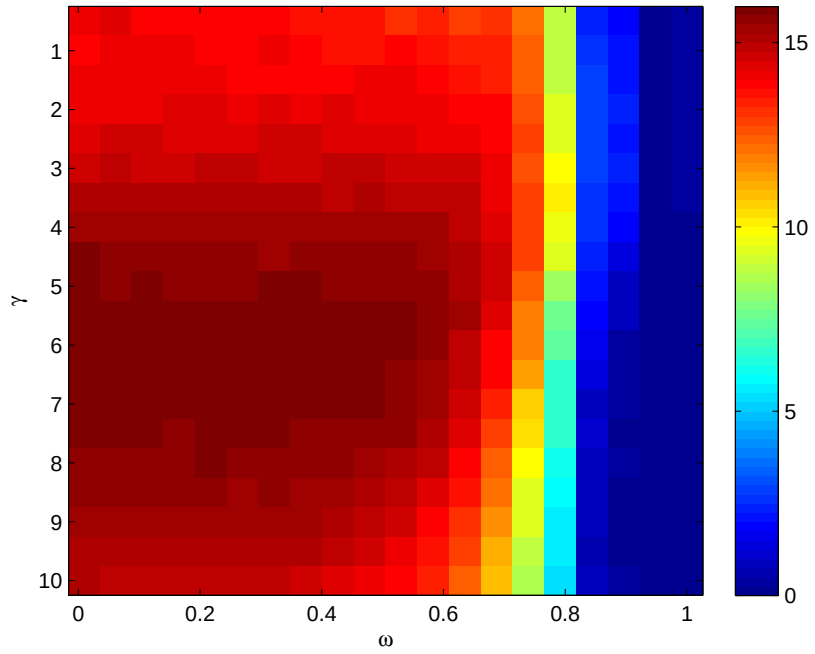

(a) flexibility measure 1

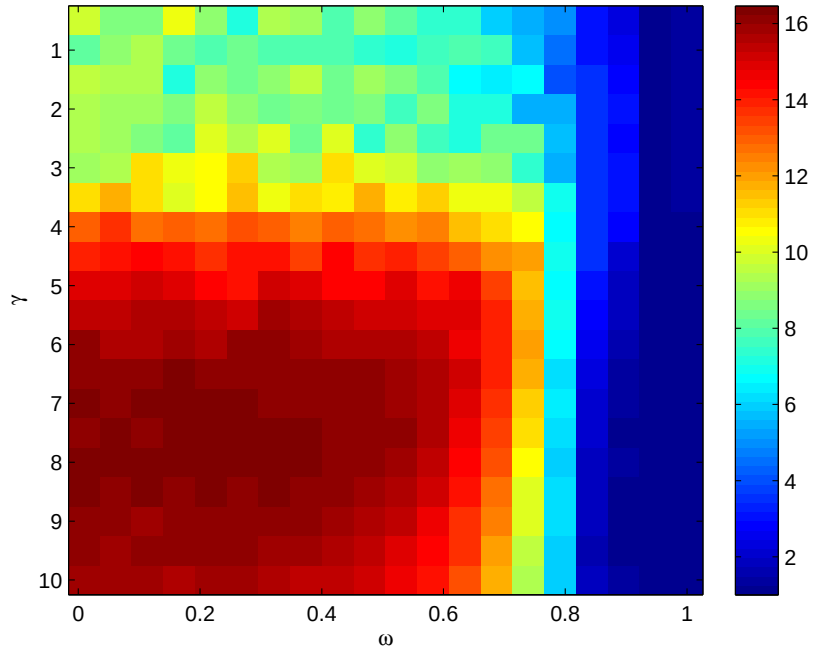

(b) flexibility measure 2

Figure 7: I tested the robustness of both measures of flexibility over a range of values of γ and ω. These are parameters in the multilayer model of community detection [18]. I chose values of γ and ω that gave reasonable community structure. It can be seen for both measures of flexibility that the value of flexibility is robust over all chosen values of ω, while the measure flexibility 2 is not robust for $\gamma \in [0.5, 4]$.

5 Discussion

The results in Section 4 compare brain graphs from healthy versus unhealthy individuals in order to attempt to distinguish patients from controls. This was more successful with the Cambridge data because the data sets contained temporal information which allowed the more powerful tool of multilayer community detection to be used. The Cornell data, by contrast, contained correlation matrices without time series data and there were at most 4 time points per individual. This was not sufficient to distinguish between patients from controls and most vitally show that the patients regained some cognitive function at later time points. The measure of communicability could only go as far as giving some distinction between brain-damaged and healthy individuals. What is more interesting to neuroscience would be to find measures that robustly characterise a brain graph and can be used to inform what is happening in the physical system.

The was more scope for analysing the data with the Cambridge data set. Temporal adjacency matrices were constructed from the time-series data and then community detection for multilayer networks was used to assign nodes to communities. I then measured the flexibility of the nodes. Analysing time-series data opened up more complications, however, as many parameters were used in each step of the analysis - the length of time window Δ for measuring the correlation between pairs of nodes and the values of ω and γ used in multilayer community detection. It is hard to say which regions of parameter space give the most accurate reflection of the subjects undergoing fMRI scans. γ can be interpreted as the inverse time for a random walk across the network, so there is some natural intuition for how γ affects community detection. The effects of ω are harder to discern. A value of $\omega = 0$ means that there is no coupling between the network layers. A value of $\omega = \infty$ is the mean-field description in which there is an average coupling between the same node over all layers. What effects ω has on the network at values in between is less certain. Ideally a more thorough investigation on how the choice of Δ, γ and ω influences the results should be conducted.

The results from the Cambridge data show that controls have a higher flexibility than patients regardless of which medication they are on (Sulpiride, Aripiprazole, or placebo). Additionally, the difference in flexibility between patients and controls was consistently larger for those on Aripiprazole compared to those taking Sulpiride or a Placebo. Aripiprazole has been prescribed to patients in the US for over 10 years [10], whereas Sulpiride is a comparatively newer drug. Sulpiride has been found in studies to have fewer extrapyramidial side effects, such as dystonia, parkinsonism, and akathisia, than older antipsychotic drugs [12]. The extrapyramidial system is defined group of structures in the brain that are involved in motor function [20]. This is something to consider when analysing fMRI data from patients taking Arip-

iprazole. What could be useful when analysing such a data set like the one from Cambridge would be some accompanying documentation detailing any side effects that the subjects may be experiencing.

5.1 Further work

My work included only a preliminary look into how the choices of parameters Δ, γ and ω affect the results. Future work should focus on this in order to discern which results are robust, rather than artefacts of the parameters used.

I conducted time ordered community detection on the Cambridge data by comparing time-dependent network layers taken from the same individual. Another approach would be to consider couplings between individuals (a multiplex network). If both the time dependent inter-individual *and* intra-individual couplings are included, then the community detection would have to be reformulated to deal with rank-4 tensors.

6 Conclusion

This report details an investigation on fMRI BOLD signal data from healthy and unhealthy individuals using network science. I found that temporal information was necessary for characterising the data, which is a consequence of the brain being a dynamic system. Analysis of temporal data is more complicated than that on a static network, since there is more methodological choice and the parameter space in the methods used is large. Correlation matrices were constructed from the time series data of time window width Δ, and the GenLouvain algorithm made use of parameters γ and ω that can vary from $[0, \infty)$. More research is needed to clarify how the values of Δ, γ, and ω affect the brain graph analysis before any definitive conclusions can be made. From the preliminary studies in this report it was found that the flexibility of a network is a way of distinguishing between schizophrenic patients and controls regardless of whether they are on an antipsychotic drug (Aripiprazole or Sulpiride) or a placebo.

Acknowledgements

Many thanks to Mason Porter and Sang Hoon Lee for invaluable guidance and suggestions. Also thanks to Sudhin Shah at Cornell for help in analysing the Cornell data, and to the Nicholas D. Schiff lab for providing it. Thanks to Professor Bullmore's lab at Cambridge for their data set. I must also give credit to Peter J. Mucha

for the GenLouvain code on Netwiki, http://netwiki.amath.unc.edu/GenLouvain/GenLouvain, and to Puck Rombach for the Core-periphery code [23].

References

[1] *S. Shah (private communication 29/08/12)*.

[2] D.S. Bassett, N.F. Wymbs, M.A. Porter, P.J. Mucha, J.M. Carlson, and S.T. Grafton. Dynamic reconfiguration of human brain networks during learning. *Proceedings of the National Academy of Sciences*, 108(18):7641–7646, 2011.

[3] V.D. Blondel, J.L. Guillaume, R. Lambiotte, and E. Lefebvre. Fast unfolding of communities in large networks. *Journal of Statistical Mechanics: Theory and Experiment*, 2008(10):P10008, 2008.

[4] E. Bullmore and O. Sporns. Complex brain networks: graph theoretical analysis of structural and functional systems. *Nature Reviews Neuroscience*, 10(3):186–198, 2009.

[5] E.T. Bullmore and D.S. Bassett. Brain graphs: graphical models of the human brain connectome. *Annual review of clinical psychology*, 7:113–140, 2011.

[6] J.J. Crofts and D.J. Higham. A weighted communicability measure applied to complex brain networks. *Journal of The Royal Society Interface*, 6(33):411–414, 2009.

[7] JJ Crofts, DJ Higham, R. Bosnell, S. Jbabdi, PM Matthews, TEJ Behrens, and H. Johansen-Berg. Network analysis detects changes in the contralesional hemisphere following stroke. *NeuroImage*, 54(1):161–169, 2011.

[8] E. Estrada and N. Hatano. Communicability in complex networks. *Physical Review E*, 77(3):036111, 2008.

[9] G. Flandin, F. Kherif, X. Pennec, D. Rivière, N. Ayache, and J.B. Poline. Parcellation of brain images with anatomical and functional constraints for fmri data analysis. In *Biomedical Imaging, 2002. Proceedings. 2002 IEEE International Symposium on*, pages 907–910. IEEE, 2002.

[10] U.S. Food and Drug Administration. `http://www.fda.gov/Safety/MedWatch/SafetyInformation/SafetyAlertsforHumanMedicalProducts/ucm153025.htm`.

[11] C.R. Genovese, N.A. Lazar, and T. Nichols. Thresholding of statistical maps in functional neuroimaging using the false discovery rate. *NeuroImage*, 15(4):870–878, 2002.

[12] J. Gerlach, K. Behnke, J. Heltberg, E. Munk-Anderson, and H. Nielsen. Sulpiride and haloperidol in schizophrenia: a double-blind cross-over study of therapeutic effect, side effects and plasma concentrations. *The British Journal of Psychiatry*, 147(3):283–288, 1985.

[13] D.J. Higham, G. Kalna, and M. Kibble. Spectral clustering and its use in bioinformatics. *Journal of computational and applied mathematics*, 204(1):25–37, 2007.

[14] B. Horwitz. The elusive concept of brain connectivity. *NeuroImage*, 19(2):466–470, 2003.

[15] R. Lambiotte, J.C. Delvenne, and M. Barahona. Laplacian dynamics and multiscale modular structure in networks. *Arxiv preprint arXiv:0812.1770*, 2008.

[16] M.E. Lynall, D.S. Bassett, R. Kerwin, P.J. McKenna, M. Kitzbichler, U. Muller, and E. Bullmore. Functional connectivity and brain networks in schizophrenia. *The Journal of Neuroscience*, 30(28):9477–9487, 2010.

[17] A.V. Mantzaris, D.S. Bassett, N.F. Wymbs, E. Estrada, M.A. Porter, P.J. Mucha, S.T. Grafton, and D.J. Higham. Dynamic network centrality summarizes learning in the human brain. *Arxiv preprint arXiv:1207.5047*, 2012.

[18] P.J. Mucha, T. Richardson, K. Macon, M.A. Porter, and J.P. Onnela. Community structure in time-dependent, multiscale, and multiplex networks. *Science*, 328(5980):876–878, 2010.

[19] M. Newman. *Networks: an Introduction*. Oxford University Press, Inc., 2010.

[20] BrainInfo University of Washington. `http://braininfo.rprc.washington.edu/centraldirectory.aspx?type=a&ID=623`.

[21] T. Prescott. Examining dynamic network structures in relation to the spread of infectious diseases, `http://people.maths.ox.ac.uk/porterm/research/TomPrescott_Project2_Final.pdf`. 2011.

[22] Human Connectome Project. `http://www.humanconnectomeproject.org/`.

[23] M.P. Rombach, M.A. Porter, J.H. Fowler, and P.J. Mucha. Core-periphery structure in networks. *arXiv preprint arXiv:1202.2684*, 2012.

[24] S.M. Smith, K.L. Miller, G. Salimi-Khorshidi, M. Webster, C.F. Beckmann, T.E. Nichols, J.D. Ramsey, and M.W. Woolrich. Network modelling methods for fmri. *NeuroImage*, 54(2):875–891, 2011.

[25] R.W. Williams and K. Herrup. The control of neuron number. *Annual Review of Neuroscience*, 11(1):423–453, 1988.